Gas-Dynamic Features of Jets Generated by Colliding Surface Discharges

Ivchenko A.V.

Samara State Aerospace University, Samara, Russia

Spatially oriented gas jets are widely used in various fields of science and engineering such as: aerodynamics, plasma-chemistry and et al. Among jet flows, it can discriminate the streams which excited by surface discharges [1]. The movement medium implementation by means electro-thermo-gas-dynamic effects [2] simplifies design of jet-device and opens new opportunities for gas flow controlling in near-wall area. However, to improve the efficiency of these devices it is necessary to find optimal electro-physical parameters for plasma actuators. In addition, there is a need to reveal relationship between the discharge modes, the jet pattern and their gas-dynamic properties at plasma excitation [3].

The studies of jet formation in quiescent air at atmospheric pressure have been carried out for electrode systems with planar geometry [4]. The flow with 2D-characteristics can be obtained this way [3]. In Fig 1 the electrode systems parameters are similar to the data of [4]. However, in contrast to [4,5], the peripheral discharge was implemented on the lower dielectric surface. It allows excluding the possibility to form a stream from peripheral discharge without changes of power consumption.

Qualitative jet analysis has been produced on the basis of smoke visualization of the flow lines, as well as changes in the density medium on shadow images [5, 7]. Quantitative information about stream has been obtained as a result of consistent application of PIV and LDA. The practical use of these methods give information not only on the averaged flow parameters, but also about its pulsations [6,7].

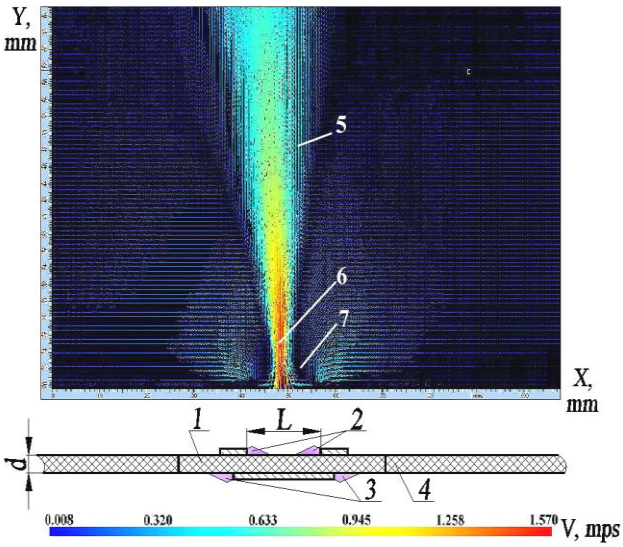

Fig.1 PIV recoding of flow formation under colliding surface discharges action at U_a=7.5 kV: 1- electrode system (L=20 mm, d=0.8 mm); 2- colliding surface discharges; 3-peripheral discharge; 4-wall; 5-gas jet; 6 –exit jet region; 7-vortex zone. L-inter-electrode gap width; d–dielectric layers thickness

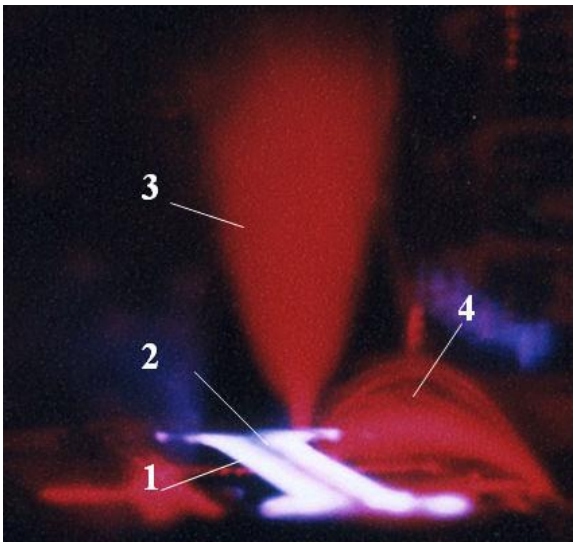

Fig. 2. Smoke visualization of gas jet normally oriented to the exposed surface of electrodes system: 1- plasma glow of colliding surface discharges; 2-dark zone into inter-electrode gap; 3-turbulent jet; 4-near-wall laminar supply stream

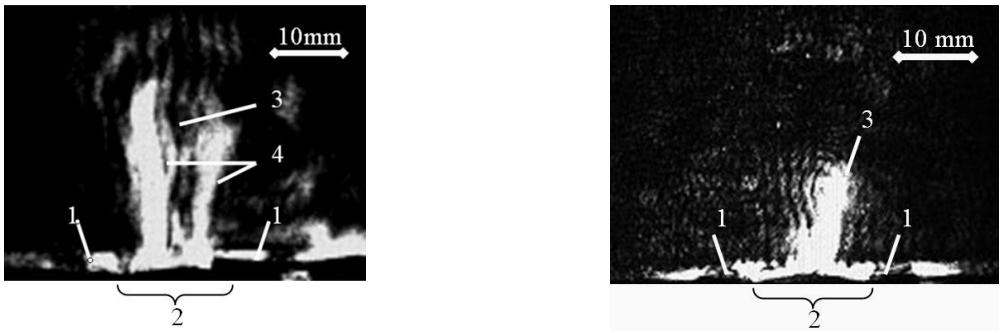

Fig.3 Shadow visualization of gas jet formation at U_a=7.5 kV in electrode system with different inter-electrode gap length: a) -d=0.8 mm, L=20 mm; b)-d=0.5 mm, L=20 mm. 1-discharege electrode; 2- inter-electrode gap; 3-heted jet. (Frame rate during video-registration was 200 fps)

At the same time, the oscilloscopic recording has been made to check the active power discharge.

The discharge formation has occurred under the influence of an alternating voltage ($dU/dt \cong 10^9$ V/s) at the amplitude U_a = 2-7.5 kV and frequency $f \cong 9$ kHz. The electrode system was placed in the wall (see Fig. 1), and according to [8], experimental unit was protected from natural convection by shields.

In Fig.1-3 there are shown the results of jets visualization by optical method. According to Fig. 1-2, the gas outflow is stared directly from the dark area located between the colliding plasma sheets. In spite of small flow speed (V<1.6 mps), Fig. 2 indicates a high degree of jet turbulence. This fact is confirmed by the seeding jet uniformity by smoke particles due to turbulence mixing. Gas suction into jet is realized via boundary layers (see in Fig.3 a). As a result of this process, the jet expansion and gradual reduction of gas stream velocity in accordance to the Momentum Conservation Law [10] are observed. Also, by analyzing Fig.1, it is possible to allocate an exit part of jet where the flow rate is constant.

It is known [10], that the gas-dynamic features of exit jet region define the subsequent processes of jet propagation in the space. So PIV-method (in the jet exit region) was used to determine the time-averaged flow speeds under conditions of changes in geometry of the electrode system (L, d), and the amplitude of the applied voltage U_a (Fig. 4-5).

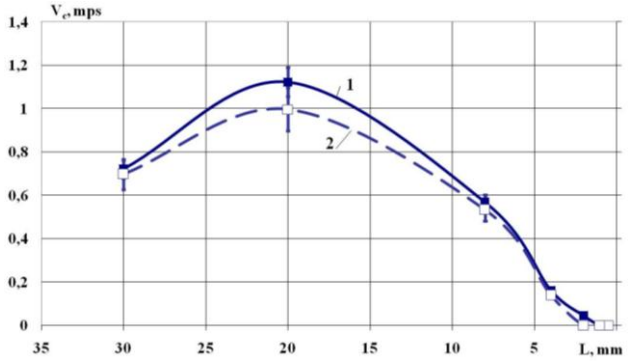

Fig.4. Dependency of jet velocity V_c in exit region from inter-electrode gap length L: 1-dielectric thickness d=0.8 mm; 2-d=1.5 mm (The alternative voltage amplitude was U_a=6.5±0.3 kV)

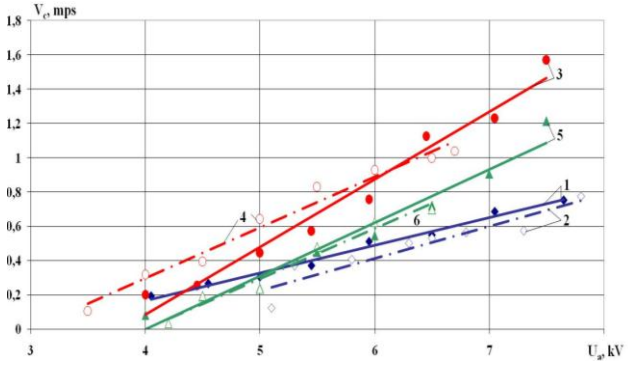

Fig.5. Dependency of jet velocity V_c in exit region from alternative voltage amplitude U_a at different parameters of electrode system: 1-d=0.8 mm, L=8 mm; 2-d=1.5 mm, L=8 mm; 3-d=0.8 mm, L=20 mm; 4-d=1.5 mm, L=20 mm; 5-d=0.8 mm, L=30 mm; 6-d=1.5 mm, L=30 mm

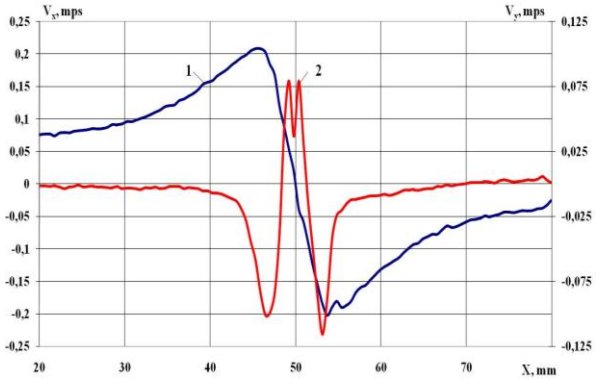

Fig.6. Transversal distributions of normal V_y and tangential V_x stream velocity components at U_a=6.5±0.3 kV and y=2.5 mm components for electrode system with d=0.8 mm, L=8 mm: 1- V_x; 2- V_y

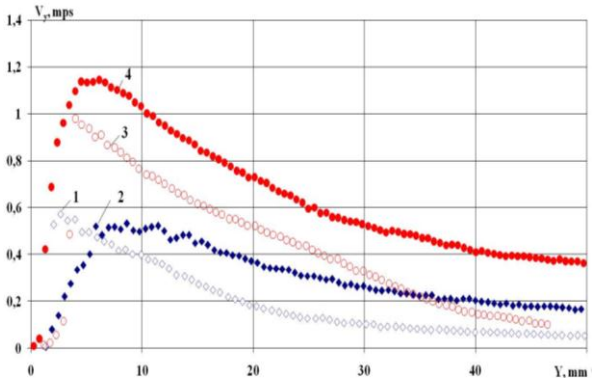

Fig.7. Axial distributions of normal velocity component V_y at U_a=6.5±0.3 kV : 1- d=1.5 mm, L=8 mm; 2 - d=0.8 mm, L=8 mm; 3-d=1.5 mm, L=20 mm; 4-d=0.8 mm, L=20 mm

The measurements were performed by means of Flow Sens–2M camera with frame frequency f_{fr}=8 Hz and laser irradiation impulse energy $W_{им}$ =30 mJ (laser Solo-120XT, λ=532 nm). The recorded images (256 frames in each series) were processed using a cross-correlative algorithm with sampling window of size 16*16 pixels and 50% overlap [6].

The obtained results (Fig. 4, 5) demonstrate the enhancing flow if the width L and voltage amplitude U_a increases (the width - up to L = 20 mm). In Fig.5 we have shown also that the experimental data can be satisfactorily approximated by linear functions in correspondence with data [3].

Spatial structure of the induced jets is represented by transverse and axial distributions of velocity components (Fig.6,7). At d = 1.5 mm, transversal flow distribution is similar to the data of [1, 3]. However, when gas discharge system with d = 0.8 mm is used, there are two peak in center of inter-electrode gap (see Fig. 6) in the distribution of the normal velocity component near the exposed dielectric surface (y <5 mm). The influence of electrode system parameters (L and d) on the axial velocity distribution can be estimated from Fig. 7. The curves in Fig. 7 show that the flow at different distances from the dielectric surface is accelerated (y <3-5 mm), then it forms the exit region (y = 5-10 mm), and after that jet is decelerated (y> 6-12 mm). For electrode systems with d = 0.8 mm, there is a significant increase in the longitudinal dimensions of the exit jet part and a slower velocity reduction in comparison with situation when d = 1.5 mm.

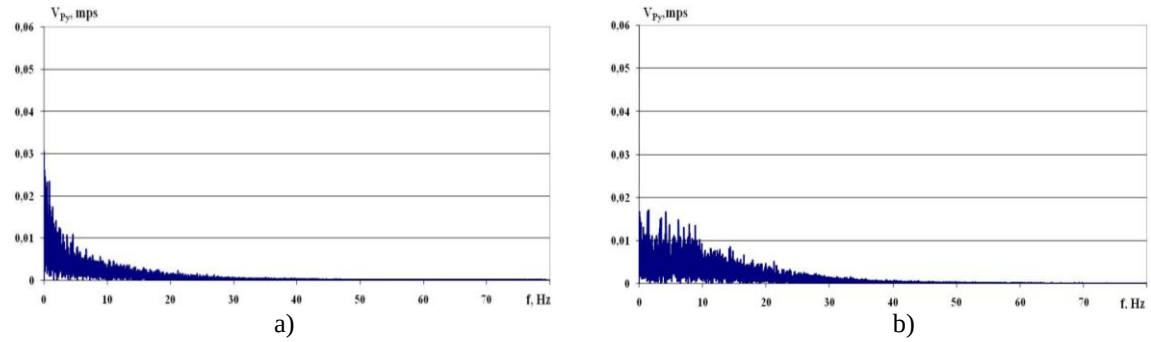

Fig. 8. Typical spectral distribution of axial flow pulsations for different points of inter-electrode gap to the near-wall area (height magnitude 1 mm): a)-over discharge electrode edge; b) –abave dark zone (see Fig.2).

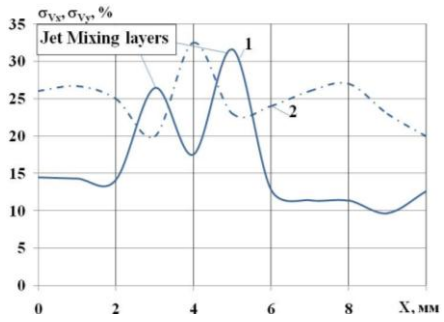

Fig.9. Turbulence intensity components distribution in the near-wall area (at height magnitude 1 mm) for electrode system with L=8 mm, d=0.8 mm (U_a=6.5 kV): 1-axial component σ_{Vx}; 2-transversal component σ_{Vy}

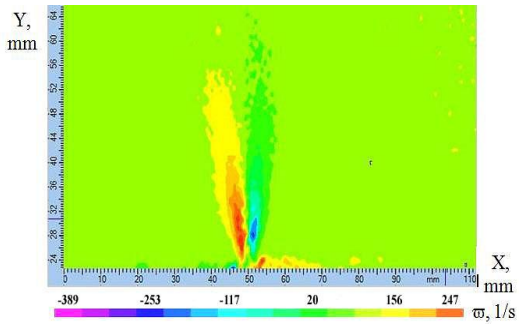

Fig.10. Jet vorticity distribution at voltage amplitude U_a=6.5 kV. Parameters of electrode system: L=8 mm, d=0.8 mm.

Pulsation flow properties are presented in Fig.8 and 9. The analysis was carried out on the basis of the ensemble containing 4096 Doppler's flares, which were registered by laser device (LAD-056). The data confirm that the gas jet has a high degree of turbulence, which reaching 30-40% (Fig. 9). The maximums of axial pulsations according to [10, 11] are located in the formation zone of the boundary layers (see Fig. 3), and coincide with the zone of high vorticity (Fig. 10).

Spectral studies showed that the pulsations spectrums are continuous (Fig. 8) and are arranged in the frequency band of 30-60 Hz. Pulsating spectrums at various points of inter-electrode gap are different in structure. Spectrums obtained near electrode working edge are decaying functions (Fig. 8 a). In the center of inter-electrode gap the spectrum distribution has a local maximum (Fig.18 b). Based on these data it is possible to conclude that various points of inter-electrode gap have the difference into energy flow scattering, as well as there is disturbances source in central part of gap L.

The scientific work was executed by support of Samara Region Grant in field of Science and Engineering.

References

[1] Santhanakrishnan A. Jacob J. D. // Journal of Physics D: Applied Physics 2007.-V.40, P. 637-651.

[2] Jayaraman B., Shyy W. // Progress in Aerospace Sciences 2007.- V. 44., i.3-P 139-191

[3] Benard N., Jolibois J., Moreau E. et al // Thin Solid Films -2008. - V.516, i.19 - P.6660-6667.

[4] Ivchenko A.V., Timchenko P.E., Zakharov V.P., et al // Europhysics Conference Abstracts - 2012.- V. 36F-4p.

[5] Ivchenko A.V. Zhuravliov O.A. Shakhov V.G. //Vestnik SSAU-2012.-№5 (36), Part 1.- P.24-33.[in Russian].

[6] Raffel M., Willert C., Kompenhans J. Particle Image Velocimetry: a practical guide – Berlin: Springer, 1998. -253 p.

[7] Dubnischev Yu. N. Laser Doppler's measuring Technologies –Novosibirsk: Publishers of NSTU, 2002.-416p. [in Russian].

[8] Belozerov A.F. Optical methods for gas flows visualizations– Kazan- Publishers of KSTU, 2007.-747p. [in Russian].

[9] Litvinenko M.V. // PhD thesis –Novosibirsk: NSTU, 2005.- 124p. [in Russian].

[10] Turbulent jets theory / G. N. Abramovich at al –Moscow-"Nauka" press-1984.716p. [in Russian].

[11] Hinze J. O. Turbulence an introduction to its mechanism – New York at al- McGraw-Hill Book Company, Inc, 1959. -680p.